Characteristic of microscopic shape memory effect in a CuAlNi alloy by nanoindentation

CHENG LIU*
State Key Laboratory of Nonlinear Mechanics, Institute of Mechanics, Chinese Academy of Sciences, 15 Zhongguancun Road, Beijing 100080, China; State Key Laboratory of Surface Physics, Institute of Physics, Chinese Academy of Sciences, P.O. Box 603, Beijing 100080, China
E-mail: cliu@aphy.iphy.ac.cn

YAPU ZHAO
State Key Laboratory of Nonlinear Mechanics, Institute of Mechanics, Chinese Academy of Sciences, 15 Zhongguancun Road, Beijing 100080, China

QINGPING SUN, TONGXI YU
Department of Mechanical Engineering, Hong Kong University of Science and Technology, Clear Water Bay, Kowloon, Hong Kong, China

ZEXIAN CAO
State Key Laboratory of Surface Physics, Institute of Physics, Chinese Academy of Sciences, P.O. Box 603, Beijing 100080, China

Shape memory alloys (SMA) can recover large inelastic strains, up to 8% tensile strain for NiTi alloys and 4% for CuAlNi alloys, either by heating (shape memory effect, SME) or by stress removal (superelasticity, SE). Both are the result of martensitic phase transformation. Recently, SMA and their thin films have been exploited for micro electromechanical systems and novel medical devices [1–3], so there is an increasing interest in probing mechanical properties of SMA by micro- and naonoindentation techniques [4–7]. It is known that the indentation of materials creates high stress under diamond indenters that can cause stress-induced phase transformation [8–10]. Ni *et al.* [5] examined the thermally induced recovery of microindents in NiTi alloys. It was found that the deformation in spherical microindents could be almost completely reversed by moderate heating. However, partial recovery was observed for Vickers impressions. In the present study, we examined the thermally induced recovery of nanoindents made at room temperature by a Berkovich indenter in both austenite (A) and martensite (M) phases of a CuAlNi single crystal SMA. The recovery behavior was scrutinized at temperatures of 40, 70 and 100 °C, respectively. It was found that the recovery ratio was sensitive to the temperature, and a large recovery ratio up to 0.7–0.9 could be achieved at 100 °C under the maximum indentation loads restricted below 10,000 μN.

A CuAlNi (Cu-14wt.%Al-4.12wt.%Ni) single crystal SMA was investigated in this research. The characteristic transformation temperatures were measured by differential scanning calorimeter (DSC 92, SETARAM, France) as: $M_s = 0.5$ °C, $M_f = -3$ °C, $A_s = 26$ °C and $A_f = 36$ °C. At room temperature, the sample exhibited SME. *A* and *M* phases could coexist in the sample by either loading–unloading or first heating to the temperature above A_f and then cooling to the temperature above M_f. The sample was mechanically polished and finished with 0.05 μm Al_2O_3 suspension. Nanoindentation tests were performed on a triboindenter with temperature controlled from 22 to 120 °C (Hysitron Inc.) and the maximum indentation load capacity of the instrument is 10,000 μN. A Berkovich indenter with roughly 150 nm tip radius was used. Nanoindentation was conducted at room temperature with the maximum load preset at 10,000, 5000 and 1000 μN, respectively. The tested area was marked with scratches to facilitate the location of indents for the *in-situ* imaging, for which the indenter was operated in the atomic force microscopy (AFM) mode. The recovery of the nanoindents was monitored after the sample had been held at 40, 70 and 100 °C for over 15 min till no more change in the indent profile could be detected.

Figs 1 and 2 show the *in-situ* AFM images of nanoindents in both phases before and after heating to 100 °C. All the imprints maintained at room temperature manifest very sharp profile, as shown in Figs 1a and 2a. With increasing temperature, the bottom of the indents turns out blurred. The figures for the indents recovery at 40 and 70 °C are not shown here. At 100 °C, the bottom corners of indents made at all the given loads are almost completely flattened (Figs 1b and 2b). In Fig. 2(b), it is also found that the macro-martensitic bands that existed at room temperature disappear after heating to temperature above A_f. During indentation, a stress-induced martensitic transformation occurred in A phase or a stress-induced martensite reorientation occurred in M phase below the indenter [9]. After prolonged heating, here the three temperatures are all above A_f, the residual deformation induced by the indentation could be recovered through a reversed phase transformation

*Author to whom all correspondence should be addressed.

0022–2461

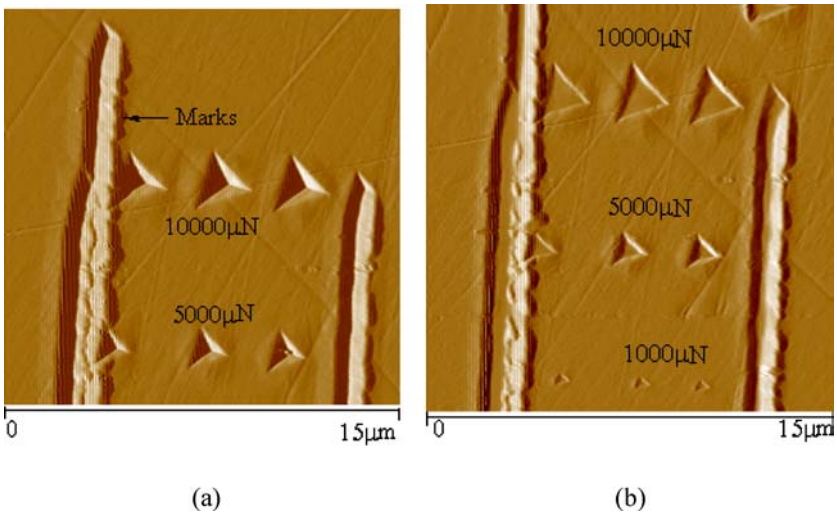

Figure 1 AFM images of the nanoindents in A phase: (a) maintained at room temperature and (b) recovered at 100 °C.

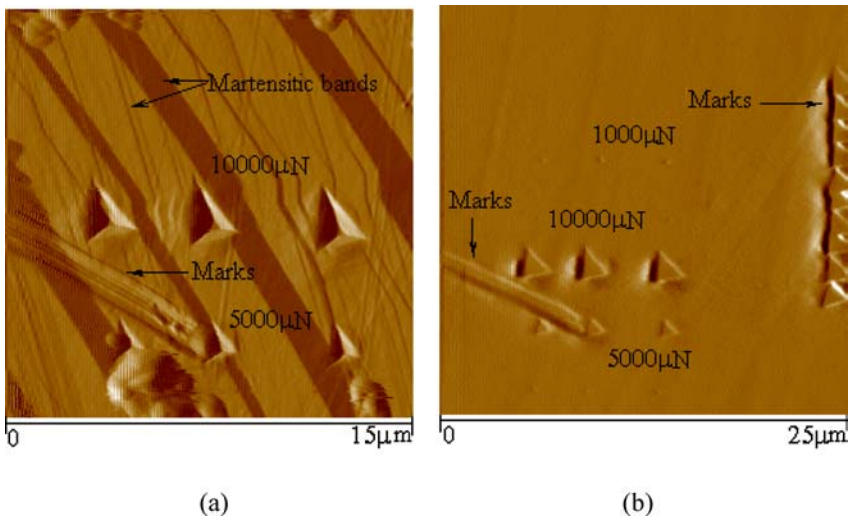

Figure 2 AFM images of the nanoindents in M phase: (a) maintained at room temperature and (b) recovered at 100 °C.

(M→A). Line scan profiles across the indents made at a maximum load of 10,000 μN and recovered at given temperatures are presented in Fig. 3. Recovery of the indents in the depth direction is evident. With increasing temperature, the indents become shallow and blunt. Thus, the shape memory effect in the CuAlNi alloy is confirmed at the microscopic level. The degree of indent recovery in the depth direction is determined quantitatively from the line scan profile by defining a recovery ratio, δ_D, as in [5]:

$$\delta_D = \frac{D_{max}^{T_0} - D_{max}^{T}}{D_{max}^{T_0}}, \quad (1)$$

where D_{max} is the maximum residual indent depth after removal of the load, and the superscripts T_0 and T refer to room temperature and heating temperature, respectively. The recovery ratios appeared to be temperature dependent. At 40 °C, δ_D lies within 0.1–0.3 for the indents made under all the applied loads. At 70 °C, δ_D is 0.4–0.7 and at 100 °C δ_D is 0.7–0.9. The residual imprints could not recover completely although the heating temperatures were all higher than A_f. During indentation, the volume of material directly under a sharp pyramidal indenter is so highly strained that significant inelastic deformation occurred by dislocation motion as well as a stress-induced phase transformation. The volume dominated by dislocation-induced deformation would not only fail to recover, but could also inhibit shape recovery strain in the underlying materials. Gall *et al.* [10] found that the induced dislocations in the Vickers microindents of NiTi alloys could stabilize stress-induced martensite plates even when the temperature above A_f. On the other hand, for comparison, one notices that the δ_D for Vickers microindents in NiTi alloys has a value of only about 0.3 in Ni *et al.*'s results [5], there the maximum load was adjusted between 50 and 2500 mN corresponding an indent depth above 500 nm, and the recovery temperature is as high as 150 °C. Their Berkovich indents recovery ratio is also as low as 0.4 [5, 6]. For ideally sharp pyramidal indenters, no length scale is involved in describing the indenter geometry. Consequently, for Berkovich and Vickers indentation in elastic–plastic solids the recovery ratio is independent of indentation load or depth [5]. However, the maximum load applied in our study was restricted below 10,000 μN, thus the resulting indent depth was only within 200 nm, being comparable to the

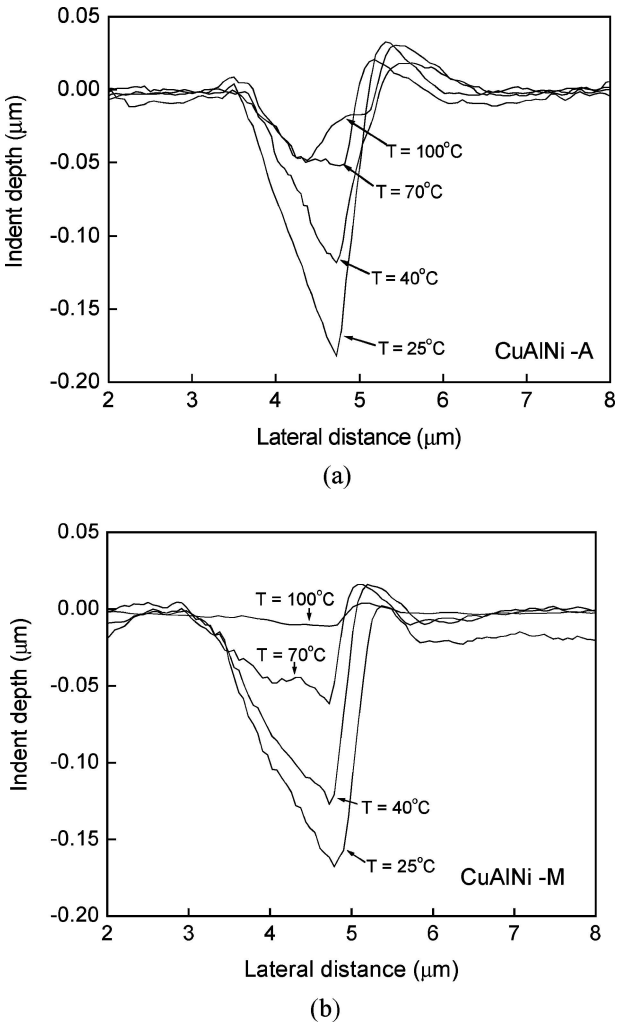

Figure 3 Line scan profiles across the indents maintained at different temperatures in both (a) A and (b) M phases. Maximum load for the indentation is 10,000 μN.

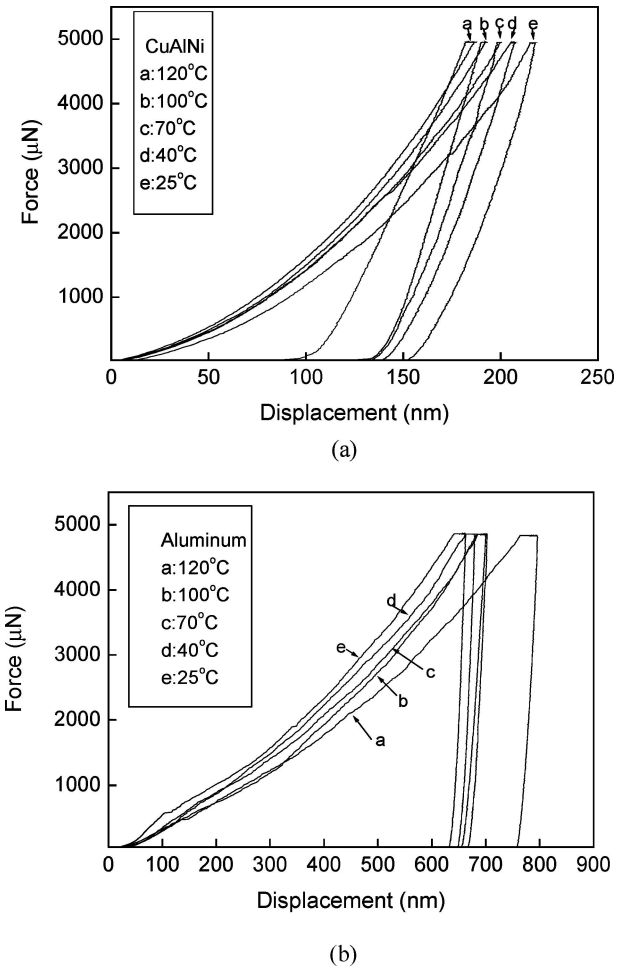

Figure 4 Force–displacement plots at different temperatures for: (a) CuAlNi single crystal and (b) Al single crystal.

radius of the blunt indenter. The recover ratio should show only slight deviation from that of spherical indentations. Under such a circumstance, the shape recovery strain dominates over the dislocation-induced plastic strain, hence a high recovery ratio is anticipated.

We also performed nanoindentation in CuAlNi at temperatures ranging from 25 to 120 °C (Fig. 4a). It is found that the maximum indentation depth decreases with increasing temperature. For comparison, indentation of an aluminum single crystal standard sample provided by Hysitron was performed (Fig. 4b). The Al single crystal has a reverse trend. The obtained nanohardness of CuAlNi at 120 °C is twice as high as that at room temperature, while the nanohardness of Al slightly decreases with increasing temperature. It is well known that hardness is a measure of the material's yield strength. The obtained data imply that the yield strength of Al slightly decreases with increasing temperature. For 1100Al, the yield strength at room temperature is about 26.1 MPa and it drops to 19.8 MPa at 126 °C [11]. Plastic deformation via dislocation motion occurred during indentation of Al. The dislocation motion at high temperature leads to the drop of yield strength, thereby resulting in the drop of hardness. As for CuAlNi, both a stress-induced phase transformation and dislocation activity occurred during indentation, so they both contributed to the variation in hardness. In the analysis of Al, it could be inferred that dislocation activity would decrease the hardness of CuAlNi with increasing temperature, so the phase transformation would contribute a lot to the increase of hardness. In many experiments [12, 13], it is found that the stress for A $\rightarrow$ M transformation increases with increasing temperature while the yield strength of M phase is nearly kept, so the average stress level in CuAlNi increases with increasing temperature. Again, it proves that when the indentation depth is comparable to the radius of blunt indenter, the significant deformation occurred by phase transformation rather than by dislocation motion in the volume of material under the indenter.

Acknowledgments

The research project is supported by the Joint Lab on Microsystems between the Institute of Mechanics, CAS and the Hong Kong University of Science and Technology (HKUST) under a HKUST fund grant number CMI00/01.EG02. The authors gratefully acknowledge Mr. William Chi Chung Wong and Mr. Peter Ka Chun Lee of HKUST for their kind help in nanoindentation work.

References

1. K. OTSUKA and T. KAKESHITA, *MRS Bulletin* **27** (2002) 91.
2. T. W. DUERIG, *ibid.* **27** (2002) 101.

3. T. W. DUERIG, A. R. PELTON and D. STOCKEL, *Bio-Med. Mater. Eng.* **6** (1996) 255.
4. W. Y. NI, Y. T. CHENG and D. S. GRUMMON, *Appl. Phys. Lett.* **82** (17) (2003) 2811.
5. W. Y. NI and Y. T. CHENG, *ibid.* **80** (18) (2002) 3310.
6. W. Y. NI, Y. T. CHENG and D. S. GRUMMON, *Surf. Coat. Technol.* **177/178** (2004) 512.
7. Y. G. GOGOTSI and V. DOMNICH, *J. Mater. Res.* **15** (4) (2000) 871.
8. V. DOMNICH and Y. G. GOGOTSI, *Rev. Adv. Mater. Sci.* **3** (2002) 1.
9. C. LIU, Q. P. SUN, Y. P. ZHAO and T. X. YU, *Int. J. Nonlinear Sci.* **3** (2002) 535.
10. K. GALL, K. JUNTUNEN, H. J. MARIER, H. SEHITOGLU and Y. I. CHUMLYAKOV, *Acta Mater.* **49** (2001) 3205.
11. Metals Handbook, Properties and Selection: Nonferrous Alloys and Pure Metals, ninth edition, Vol. 2 American Society for Metals (Metals Park, Ohio 44073, 1979) p. 67.
12. H. SAKAMOTO, K. SHIMIZU and K. OSTUKA, *Trans JIM* **26** (9) (1985) 638.
13. K. OSTUKA, H. SAKAMOTO and K. SHIMIZU, *Acta Metall.* **27** (1979) 585.

Received 27 May
and accepted 20 July 2004